Thermo-Viscoelastic Residual Stress Analysis of Metal Liner-Inserted Composite Cylinders

Ho Yon Hwang
Department of Aerospace Engineering, Sejong University, Seoul 143-747, Korea
Yeong Kook Kim
Georgia Tech Research Institute, Atlanta, Georgia, 30332, USA
Cheol Kim*, Young-Doo Kwon, Woong Choi
Department of Mechanical Engineering, Kyungpook National University, Daegu 702-701, Korea

One of the most significant problems in the processing of composite materials is residual stress. The high residual stress may cause cracking in the matrix without external loads and degrade the integrity of composite structures. In this study, thermo-viscoelastic residual stresses occurred in an aluminum liner-inserted polymer composite cylinder are investigated. This type of the structure is used for rocket fuselage due to the convenience to attach payloads and equipment to the metal liner by machining. The time and degree of cure dependent thermo-viscoelastic constitutive equations are developed and coupled with a thermo-chemical process model. These equations are solved with the finite element method to predict the residual stresses in the composite cylinder and also in the interface between the liner and the composite during cure.

Key Words : Composite Cylinder, Cure-Induced Residual Stress, Thermo-Viscoelastic Analysis, Finite Element Analysis, Liner

1. Introduction

Processing-induced residual stress in fiber-reinforced composite materials is one of factors that adversely affect strength. This residual stress is caused by the difference of the thermal expansion coefficients of fiber and matrix, the large temperature gap between cure and cool-down, and the chemical shrinkage from cross-linking reactions of polymer during cure. The residual stress may induce cracks in matrix even under relatively low mechanical loads and result in the degradation of strength.

A number of analyses to predict residual st-

* Corresponding Author,
E-mail : kimchul@knu.ac.kr
TEL : +82-53-950-6586; FAX : +82-53-950-6550
Department of Mechanical Engineering, Kyungpook National University, 1370 Sankyuk-Dong, Book-Gu, Daegu 702-701, Korea. (Manuscript Received November 7, 2001; Revised November 7, 2002)

resses have been performed since the simple elastic work by Hahn and Pagano (1975). Wang and Crossman (1977) computed elastic free edge interlaminar stresses of composite laminates induced by temperature change. White and Hahn (1992) developed a process model predicting the residual stress history during the cure process of linear viscoelastic composite laminates. Bogetti and Gillespie (1992) analyzed the cure-induced residual stress for thick elastic laminates and investigated the effect of chemical shrinkage on the development of the residual stress. White and Kim (1998) developed viscoelastic constitutive equations depending on the degree of cure and temperature and computed the residual stress of composite laminates. Lee (2000) developed a computer program based on 3-D degenerated shell finite elements and studied the viscoelastic effect on residual stresses in a laminated shell. Kim and White (2001) fabricated a 155 mm thick filament-wound composite cylinder and investigated the

residual stress with analytical both and experimental ways. Previous works, however, are one of elastic models (Hahn and Pagano, 1975; Wang and Crossman, 1977; Bogetti and Gillespie, 1992; Kim and White, 2001), a laminated plate (White and Kim, 1998), and a shell only using viscoelastic models (Lee, 2000).

This paper addresses how the thermo-viscoelastic residual stress of aluminum liner-inserted polymer composite cylinders develop during whole processing and can be predicted. This type of a structure is used for the rocket fuselages due to its convenience to attach payloads and equipments to the metal liner by machining. The filament winding process is widely used for the manufacture of composite rocket fuselages. In actual process, there exist balanced laminates having plus and minus helical angles. A viscoelastic finite element code combined with the thermo-chemical model of a heat transfer equation and cure kinetics has been developed and validated by comparing with other numerical results. Using this code, the influences of the aluminum liner, winding angles, and stress relaxation on the development of residual stresses during the whole curing process are investigated. The cylinder used for this study is made of an aluminum 6061-T6 liner and AS4/3501-6 graphite/epoxy composites.

2. Viscoelastic Constitutive Equation

A general linear viscoelastic constitutive equation of the relaxation of residual stresses during cure is

$$\sigma_{ij}=\int_0^t Q_{ij}(\alpha, T, t-\tau)\frac{\partial}{\partial \tau}(\varepsilon_j^T(\tau)-\varepsilon_j^\Delta(\tau))\,d\tau \quad (1a)$$
$$(i, j=1, 2, \cdots, 6)$$
$$\varepsilon_j^\Delta=\beta_{jk}\Delta T_k+\kappa_{jk}\Delta\alpha_k \quad (1b)$$

where σ_{ij} is the stress components, Q_{ij} the effective stiffness, ε_j^T the total strain, ε_j^Δ the free thermo-chemical strain; β_{jk} and κ_{jk} represent the thermal expansion coefficients and the chemical shrinkage coefficients; ΔT and $\Delta\alpha$ are the temperature and degree of cure changes; t is the current time, and τ is the past time. For polymer composite materials, the mechanical properties

generally vary during manufacturing depending on the degree of cure.

If the material is thermo-rheologically simple at a constant degree of cure α_c, Eq. (1) can be rewritten as

$$\sigma_{ij}=\int_0^t Q_{ij}(\alpha_c, T_c, \xi^t-\xi^\tau)\frac{\partial}{\partial \tau}[\varepsilon_j^T(\tau)-\varepsilon_j^\Delta(\tau)]\,d\tau \quad (2)$$

where T_c represent the reference temperature. The reduced times are defined as

$$\xi^t=\int_0^t \chi[\alpha_c, T(s)]\,ds \quad (2a)$$
$$\xi^\tau=\int_0^\tau \chi[\alpha_c, T(s)]\,ds \quad (2b)$$

where χ is the shift function.

If the material is transversely isotropic in the on-axis cylindrical coordinates, the effective stiffness matrix (Vinson and Sierakowski, 1987) is

$$\begin{Bmatrix} \bar{\sigma}_z \\ \bar{\sigma}_\theta \\ \bar{\sigma}_r \\ \bar{\sigma}_{\theta r} \\ \bar{\sigma}_{rz} \\ \bar{\sigma}_{z\theta} \end{Bmatrix}=\begin{bmatrix} \bar{Q}_{11} & \bar{Q}_{12} & \bar{Q}_{12} & 0 & 0 & 0 \\ \bar{Q}_{12} & \bar{Q}_{22} & \bar{Q}_{23} & 0 & 0 & 0 \\ \bar{Q}_{12} & \bar{Q}_{23} & \bar{Q}_{22} & 0 & 0 & 0 \\ 0 & 0 & 0 & (\bar{Q}_{22}-\bar{Q}_{23})/2 & 0 & 0 \\ 0 & 0 & 0 & 0 & \bar{Q}_{66} & 0 \\ 0 & 0 & 0 & 0 & 0 & \bar{Q}_{66} \end{bmatrix}\begin{Bmatrix} \bar{\varepsilon}_z \\ \bar{\varepsilon}_\theta \\ \bar{\varepsilon}_r \\ \bar{\varepsilon}_{\theta r} \\ \bar{\varepsilon}_{rz} \\ \bar{\varepsilon}_{z\theta} \end{Bmatrix} \quad (3)$$

where,

$$\bar{Q}_{11}=\frac{1-\nu_{r\theta}\nu_{\theta r}}{\Delta}\bar{E}_z \quad (3a)$$
$$\bar{Q}_{12}=\frac{\nu_{\theta z}+\nu_{rz}\nu_{r\theta}}{\Delta}\bar{E}_z \quad (3b)$$
$$\bar{Q}_{22}=\frac{1-\nu_{rz}\nu_{r\theta}}{\Delta}\bar{E}_r \quad (3c)$$
$$\bar{Q}_{23}=\frac{\nu_{\theta r}+\nu_{zr}\nu_{\theta z}}{\Delta}\bar{E}_r \quad (3d)$$
$$\bar{Q}_{66}=\bar{G}_{12} \quad (3e)$$
$$\Delta=1-\nu_{zr}\nu_{rz}-\nu_{r\theta}\nu_{\theta r}-\nu_{\theta z}\nu_{z\theta}-2\nu_{rz}\nu_{\theta r}\nu_{z\theta} \quad (3f)$$

For an axisymmetric case, there is no displacement in the θ direction; Eq. (3) is rewritten as

$$\begin{Bmatrix} \bar{\sigma}_z \\ \bar{\sigma}_\theta \\ \bar{\sigma}_r \\ \bar{\sigma}_{z\theta} \end{Bmatrix}=\begin{bmatrix} \bar{Q}_{11} & \bar{Q}_{12} & \bar{Q}_{12} & 0 \\ \bar{Q}_{12} & \bar{Q}_{22} & \bar{Q}_{23} & 0 \\ \bar{Q}_{12} & \bar{Q}_{23} & \bar{Q}_{22} & 0 \\ 0 & 0 & 0 & \bar{Q}_{44} \end{bmatrix}\begin{Bmatrix} \bar{\varepsilon}_z \\ \bar{\varepsilon}_\theta \\ \bar{\varepsilon}_r \\ \bar{\varepsilon}_{z\theta} \end{Bmatrix}. \quad (4)$$

where the symbol over-bar '$\bar{\ }$' represents the material symmetry axes condition.

3. Effective Stiffness, Shift Function and Relaxation Time

The stress relaxation function for thermo-rheologically complex materials is modeled by a finite exponential series as

$$Q_{ij}(\alpha, \xi) = Q_{ij}^{\infty}(\alpha) + Q_{ij}^{*}(\alpha) \sum_{m=1}^{N} W_m(\alpha) \exp\left[-\frac{\xi(\alpha, T)}{\tau_m(\alpha)}\right] \quad (5)$$

where Q_{ij}^{∞} is the fully relaxed stiffness, τ_m is the relaxation times, $Q_{ij}^{*} = Q_{ij}^{u} - Q_{ij}^{\infty}$, Q_{ij}^{u}, is the unrelaxed elastic stiffness, W_m is the weight factors, and ξ is the reduced time. To simplify Eq. (5), we assume that the weight factors, W_m, are independent of the degree of cure and temperature (Kim and White, 1996). We also assume that the unrelaxed and fully relaxed stiffnesses of resin are independent of cure and temperature and the assumption is verified by stress relaxation test (Kim and White, 1996). Therefore, Eq. (5) is reduced further as

$$Q_{ij}(\alpha, \xi) = Q_{ij}^{\infty} + Q_{ij}^{*} \sum_{m=1}^{N} W_m \exp\left[-\frac{\xi(\alpha, T)}{\tau_m(\alpha)}\right] \quad (6)$$

Once the unrelaxed stiffnesses are obtained, then the effective stiffnesses can be calculated using Eq. (6). The unrelaxed stiffness Q_{ij}^{u} is the elastic stiffness of laminates and are listed in Table 1.

The shift function χ of AS4/3501-6 composite is a linear function of temperature with degree-of-cure dependent coefficients and defined as (Kim and White, 1996)

$$\log(\chi) = \left\{-1.4\exp\left(\frac{1}{1-\alpha}\right) - 0.0712\right\}(T - T_c) \quad (7)$$

where α is the degree of cure, and T_c is the reference temperature. The stress relaxation time τ_m is expressed as ;

$$\log(\tau_m) = \log(\tau_m(\alpha_c)) \\ + \{f'(\alpha) - (\alpha - \alpha_c)\log(\lambda_m)\} \quad (8a)$$

$$f'(\alpha) = f(\alpha) - f(\alpha_c) \quad (8b)$$

$$f(\alpha) = 0.0536 + 0.0615\alpha + 0.9227\alpha^2 \quad (8c)$$

$$\lambda_m = \frac{10^{9.9}}{\tau_m(\alpha_c)} \quad (8d)$$

where the reference degree of cure α_c is 0.98. For the time-dependent stiffness, the weight factor

Table 1 Mechanical properties of AS4/3501-6 in the principal material directions

Properties		Values
$\bar{Q}_{11}$	(GPa)	127.4
$\bar{Q}_{12}$	(GPa)	3.88
$\bar{Q}_{22}$	(GPa)	10.0
$\bar{Q}_{23}$	(GPa)	4.88
$\bar{Q}_{66}$	(GPa)	2.57
β_{11}	($\mu\varepsilon/°C$)	0.5
$\beta_{22} = \beta_{33}$	($\mu\varepsilon/°C$)	35.3
κ_{11}	($\mu\varepsilon$)	−167.0
$\kappa_{22} = \kappa_{33}$	($\mu\varepsilon$)	−8810.0

Table 2 Weight factor and relaxation times in Eq. (6)

W	τ_m(min)	W_m
1	2.922137×10^1	0.0591334
2	2.921437×10^3	0.0661225
3	1.822448×10^5	0.0826896
4	1.1031059×10^7	0.112314
5	2.8305395×10^8	0.154121
6	7.9432822×10^9	0.2618288
7	1.953424×10^{11}	0.1835594
8	3.3150756×10^{12}	0.0486939
9	4.9174856×10^{14}	0.0252

and stress relaxation time are listed in Table 2.

4. Thermo-Chemical Model

A thermo-chemical model is needed to calculate the temperature and degree of cure of composite materials during cure. The degree of cure is defined as the ratio of the heat of the reaction released up to time t and the total heat of the reaction. The degree of cure at time t is defined in terms of a cure rate such as

$$\alpha(t) = \int_0^t \frac{d\alpha}{dt} dt \quad (9)$$

To describe the cure rate, cure kinetic models are used. For the 3501-6 resin, the reaction kinetics are determined empirically as (Lee et al., 1982)
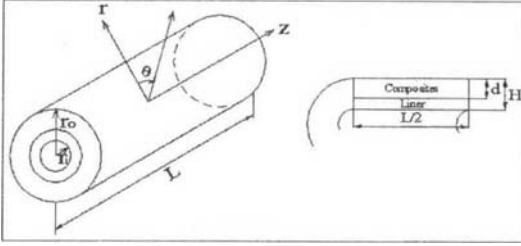
$$\frac{d\alpha}{dt} = (k_1 + k_2\alpha)(1 - \alpha)(0.47 - \alpha) \quad (\alpha \le 0.3) \quad (10a)$$

$$\frac{d\alpha}{dt} = k_3(1 - \alpha) \quad (\alpha > 0.3) \quad (10b)$$

The parameters k_1, k_2 and k_3 are defined as

Table 3　Cure kinetic parameters of AS4/3501-6

Constants		Values
A_1	(/min)	2.102×10^9
A_2	(/min)	-2.014×10^9
A_3	(/min)	1.960×10^5
ΔE_1	(J/mol)	8.07×10^4
ΔE_2	(J/mol)	7.78×10^4
ΔE_3	(J/mol)	5.56×10^4

Fig. 1　Geometries of the liner/composite cylinder

$$k_1 = A_1 \exp(-\Delta E_1/RT) \qquad (10c)$$

$$k_2 = A_2 \exp(-\Delta E_2/RT) \qquad (10d)$$

$$k_3 = A_3 \exp(-\Delta E_3/RT) \qquad (10e)$$

where R is the universal gas constant, A_1, A_2 and A_3 are the pre-exponential coefficients, and ΔE_1, and ΔF_2 are ΔE_3 the activation energies.

The corresponding boundary and initial conditions are

$$T(L/2, r, t) = T(z, d, t) = T_{cycle}(t)$$

$$\frac{\partial T(0, r, t)}{\partial z} = \frac{\partial T(z, 0, t)}{\partial r} = 0$$

$$T(z, r, 0) = T_c$$

$$\alpha(z, r, 0) = \alpha_c$$

$$0 \le r \le H, \ 0 \le z \le L/2$$

where T_c and α_c are the initial temperature and the degree of cure, respectively. The parameters used in Eq. (10) are listed in Table 3. The cylinder geometries are shown in Fig. 1.

5. Finite Element Formulation

In this section, we formulate the finite element model using the variational theorem for linear viscoelastic materials (Christensen, 1982). For an anisotropic viscoelastic material, the variation of potential energy for a finite element is given

below (Lin and Yi, 1991)

$$\delta \Pi = \int_V \int_{\tau'=-\infty}^{\tau=t} \int_{\tau=-\infty}^{\tau=t-\tau'} Q_{ij}^e[\alpha, T, t, \tau, \tau']$$

$$\frac{\partial}{\partial s}\{\varepsilon_i^e(\tau) - \varepsilon_i^{\Delta e}(\tau)\}ds \frac{\partial[\delta \varepsilon_j^e(\tau')]}{\partial \tau'} d\tau' dV \quad (11)$$

$$- \int_S \int_{\tau=-\infty}^{\tau=t} \Omega_i(t-\tau) \frac{\partial[\delta u_i(\tau)]}{\partial \tau} d\tau dS$$

where Ω_i is the surface traction, u_i is the nodal displacement and superscript e represents element quantities. The variable t is current time, and τ and τ' represent past time. S and V are an element surface area and an element volume, respectively.

The time-dependent element off-axis stiffness matrix $[Q^e]$ is defined as

$$[Q^e] = [T][\bar{Q}^e][T]^T \qquad (12)$$

where $[T]$ is the in-plane transformation matrix and $[\bar{Q}^e]$ is the element on-axis stiffness matrix. Displacements are determined from the element nodal degree of freedom $\{q_n^e\}$ as

$$\{u(t)\} = [N]\{q_n^e(t)\} \qquad (13)$$

where $[N]$ is the shape function. Strain can be calculated using the strain-displacement relations $[B]$ such that

$$\{\varepsilon_n^e(t)\} = [B]\{q_n^e(t)\} \qquad (14)$$

Assuming that there are no mechanical strain during cure, substituting Eqs. (13)-(14) into Eq. (11) and after all element matrices are assembled, the system equation yields time-superposition integration at a constant degree of cure α such that

$$\sum_{e=1}^{total} \int_{-\infty}^{t} [k_{mn}^e(\alpha, \xi - \xi')] \frac{\partial\{u(\tau)\}}{\partial \tau} d\tau$$

$$= \sum_{e=1}^{total} \left[\int_{-\infty}^{t} f_m^e(\alpha, \xi - \xi') \frac{\partial\{\varepsilon_n^{\Delta e}(\tau)\}}{\partial \tau} d\tau + f_n^e(t) \right] \qquad (15)$$

where,

$$k_{mn}^e(\alpha, \xi - \xi') = \int_V [B]^T [Q^e(\alpha, \xi - \xi')][B] dV \quad (15a)$$

$$f_m^e(\alpha, \xi - \xi') = \int_V [B]^T [Q^e(\alpha, \xi - \xi')] dV \quad (15b)$$

$$f_n^e(\xi - \xi') = \int_S [N]^T \{\Omega\} ds \qquad (15c)$$

If there are the traction force $\Omega_i(t < 0)$ and no strain when $t < 0$, and the time-dependent stiffness model Eq. (6) is used, then the Eq. (15)

becomes

$$\sum_{e=1}^{total} [k_{mn}^e(\alpha, \xi)]\{u(0)\}$$
$$+\sum_{e=1}^{total} \int_0^t [k_{mn}^e(\alpha, \xi-\xi')]\frac{\partial\{u(\tau)\}}{\partial\tau} = F_n(t)$$
(16)

where,

$$[k_{mn}^e(\alpha, \xi)] = \int_V [B]^T[Q^{e\infty}][B]dV$$
$$+\sum_{m=1}^N \int_V [B]^T\Big\{[Q^{e*}W_m]\exp\Big(-\frac{\xi^e}{\tau_m(\alpha)}\Big)\Big\}[B]dV$$
(16a)

$$[k_{mn}^e(\alpha, \xi-\xi')] = \int_V [B]^T\Big\{[Q^{e\infty}]$$
$$+\sum_{m=1}^N [Q^{e*}W_m]\exp\Big(-\frac{\xi^e-\xi^{e'}}{\tau_m(\alpha)}\Big)\Big\}[B]dV$$
(16b)

$$F_n(t) = \Big[f_n^{e\infty} + \sum_{m=1}^N f_{n_m}^{e*}\exp\Big(-\frac{\xi^e}{\tau_m(\alpha)}\Big)\Big]\varepsilon_n^{\Delta e}(0)$$
$$+\int_0^t \Big[f_n^{e\infty} + \sum_{m=1}^\infty f_{n_m}^{e*}\exp\Big(-\frac{\xi^e-\xi^{e'}}{\tau_m(\alpha)}\Big)\Big]\frac{\partial\varepsilon_n^{\Delta e}(s)}{\partial s}ds$$
(16c)

$$f_n^{e\infty} = \int_V [B]^T[Q^{e\infty}]dV$$
(16d)

$$f_{n_m}^{e*} = \int_V [B]^T[Q^{e*}W_m]dV$$
(16e)

The recursive formulation proposed by Taylor et al. (1970) is applied to handle the large computation time and storage problem. The derivative of displacement u with respect to time is approximated by

$$\frac{\partial u(t)}{\partial t} \cong \frac{u(t_j)-u(t_{j-1})}{t_j-t_{j-1}}, \ t_{j-1}\le t\le t_j$$
(17)

The thermal strain is assumed as piecewise linear during each time interval as

$$\frac{\partial\varepsilon^\Delta(t)}{\partial t} \cong \frac{\varepsilon^\Delta(t_j)-\varepsilon^\Delta(t_{j-1})}{t_j-t_{j-1}}, \ t_{j-1}\le t\le t_j$$
(18)

Degree of cure α is assumed constant during each time interval and is obtained separately by solving the thermo-chemical energy balance equations.

Using Eqs. (16)–(18), a recursive equation is formulated as

$$\bar{K}\Delta\mathbf{u}_n(t_p) = \bar{F}$$
(19)

where,

$$\bar{K} = \sum_{e=1}^{total}\Big[k_{mn}^{e\infty} + \sum_{r=1}^N k_{mn}^{e*}h_r^e(\Delta t_p)\Big]$$
(19a)

$$\bar{F} = F_n(t) - \sum_{e=1}^{total}\Big[k_{mm}^{e\infty}u_n(t_{p-1}) + \sum_{r=1}^N g_r^e(t_p)\Big]$$
(19b)

$$g_r^e(t_p) = \exp\Big(-\frac{\Delta\xi_{t_p}^e}{\tau_m}\Big)\{g_r^e(t_{p-1})$$
$$+ k_{mr}^{e*}h_r^e(\Delta t_{p-1})\Delta u_n(t_{p-1})\}$$
(19c)

$$h_r^e(\Delta t_p) = \frac{1}{\Delta t_p}\int_{t_{p-1}}^{t_p}\exp\Big(-\frac{\Delta\xi_{t_p}^e}{\tau_m}\Big)d\tau$$
(19d)

and the function values at the initial time are $g_r^e(0)=0$ and $h_r^e(0)=1$. The subscript p denotes current time. The displacement $u_n(t_p)$ is updated as

$$u_n(t_p) = u_n(t_{p-1}) + \Delta u_n(t_p)$$
(20)

Since the time-dependent stiffness depends on the degree of cure for each element, all elements have a different stiffness matrix for each time step. Assembly procedure has to be, therefore, repeated after calculating the element matrix for each time step.

The aluminum liner, in this study, is assumed to be perfectly elastic. Then, the constitutive equation of the liner is

$$\begin{Bmatrix}\sigma_z\\\sigma_\theta\\\sigma_r\\\sigma_{rz}\end{Bmatrix} = \begin{bmatrix}d_{11}&d_{12}&d_{13}&0\\d_{12}&d_{22}&d_{23}&0\\d_{13}&d_{23}&d_{33}&0\\0&0&0&d_{66}\end{bmatrix}\begin{Bmatrix}\varepsilon_z\\\varepsilon_\theta\\\varepsilon_r\\\varepsilon_{rz}\end{Bmatrix}$$
(21)

Since the liner material is isotropic, the stiffnesses are simplified as

$$d_{11}=d_{22}=d_{33}=\frac{E(1-\nu)}{(1+\nu)(1-2\nu)}=d_1$$
(21a)

$$d_{12}=d_{13}=d_{23}=\frac{E\nu}{(1+\nu)(1-2\nu)}=d_2$$
(21b)

$$d_{66}=\frac{E}{2(1+v)}=d_3$$
(21c)

And the elastic formulation is written as

$$\int_V [B]^T[D][B]\{q_n^e\}dV = \int_V [B]^T[D]\{\varepsilon_n^e\}dV$$
(22)

where $[D]$ and $\{\varepsilon_n^e\}$ represent the isotropic material property matrix and thermal strain vector of the liner elements, respectively. The material properties of the liner used in this study are listed in Table 4. In addition Eq. (19) can be expanded when including the isotropic elastic material,

Table 4 Material properties of 6061–T6 aluminum

Properties		Values
E	(GPa)	69.5
ν		0.3
d_1	(GPa)	93.6
d_2	(GPa)	40.1
d_3	(GPa)	26.7
β	$(\mu\varepsilon/^{0}C)$	23.6

$$(\bar{K}+\bar{K}^{E})\Delta\mathbf{u}_{n}(t_{p})=(\bar{F}+\bar{F}^{E}) \tag{23}$$

where,

$$\bar{K}^{E}\sum_{e=1}^{E-total}\int_{V}[B]^{T}[D][B]dV \tag{23a}$$

$$\bar{F}^{E}=\sum_{e=1}^{E-total}\int_{V}[B]^{T}[D]dV \tag{23b}$$

and the superscript E denotes elastic.

From this equation, the displacements of the cylinder are calculated and then strains are determined using the linear strain-displacement relationships in the cylindrical coordinate. Once strains are calculated, element stresses can be obtained from

$$\sigma^{e}(t)=\int_{0}^{t}Q_{ij}^{e}(\alpha,\ \xi-\xi')\frac{\partial}{\partial\tau}[\varepsilon_{j}^{Te}(\tau)-\varepsilon_{j}^{\Delta e}(\tau)]d\tau \tag{24}$$

where ε_{j}^{Te} are total strains and $\varepsilon_{j}^{\Delta e}$ are non-mechanical strains. Using the same recursive formulation, this equation can be transformed to

$$\sigma^{e}(t_{p})=\left[k_{mn}^{e\infty}+\sum_{r=1}^{N}k_{mr}^{e^{*}}h_{r}^{e}(\Delta t_{p})\right]\Delta\varepsilon_{n}^{e}(t_{p})$$
$$+k_{mn}^{e\infty}\varepsilon_{n}^{e}(t_{p-1})+\sum_{r=1}^{N}g_{r}^{e}(t_{p}) \tag{25}$$

where,

$$\Delta\varepsilon_{n}^{e}(t_{p})=\varepsilon_{n}^{e}(t_{p})-\varepsilon_{n}^{e}(t_{p-1}) \tag{25a}$$

$$g_{r}^{e}(t_{p})=\exp\left(-\frac{\Delta\xi_{t_{p}}^{e}}{\tau_{m}}\right)\{g_{r}^{e}(t_{p-1})+k_{mr}^{e^{*}}h_{r}^{e}(\Delta t_{p-1})\Delta\varepsilon_{n}^{e}(t_{p-1})\} \tag{25b}$$

It is noticed from these equations that the results only from one previous time step are enough to calculate present stresses.

6. Numerical Results

In an effort to validate the analysis and the computer code developed in this study, the numerical results from the present model are compared with other results (Lee, 2000) that were
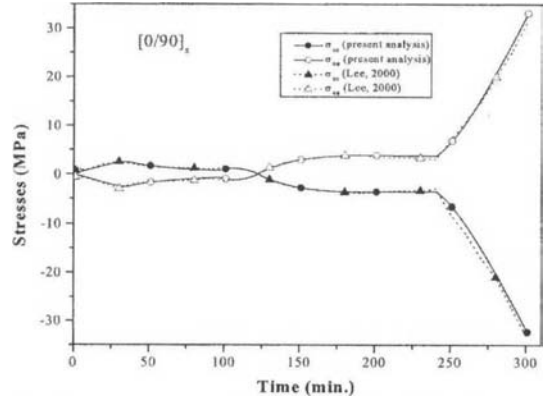

Fig. 2 Comparison of current results with other numerical solutions for longitudinal and hoop stresses
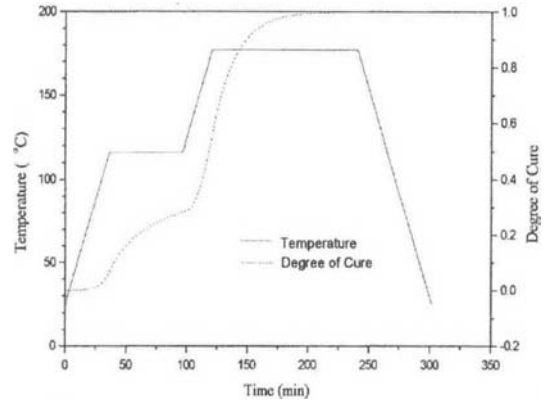

Fig. 3 Cure cycle for the composite cylinder

obtained from the analysis of a laminated semi-circular shell consisting of $[0/90]_{s}$ at the first ply and near the center using 3-D degenerate shell elements during the whole cure time of 300 minutes. The radius, length, and thickness of the shell are 100 mm, 200 mm, and 2 mm, respectively. All four edges were set to be free. The two results show an excellent agreement throughout the curing process as in Fig. 2. The good correlation of two results validates the accuracy of the present method to predict residual stress.

Numerical analyses are performed for the composite cylinders with three winding patterns such as $[(15/-15)_{2s}/90_{4}]$, $[(30/-30)_{2s}/90_{4}]$, and $[(45/-45)_{2s}/90_{4}]$ over the entire cure cycle. The outer four layers of hoop winding are added to reinforce the stiffness in the circumferential direc-

tion. The geometries of the liner/composite cylinder used for numerical studies are shown in Fig. 1. Due to the symmetry, only the half is considered. The perfect bonding between the composite layer and the aluminum liner is assumed. The isoparametric ring finite elements are used for modeling the cylindrical structure. node. The 8 degree of freedom element of this study has four nodes. The cure cycle used is shown in Fig. 3. The values of the dimension are as follows :

$$L=600 \text{ mm}, \quad H=2.5 \text{ mm}, \quad d=1.5 \text{ mm}$$

$$r_o=160 \text{ mm}, \quad r_i=157.5 \text{ mm}$$

Aluminum Liner Thickness=1 mm

Composite Thickness=1.5 mm

In Figs. 4-6 the residual stresses through the cylinder wall thickness at $z=0$, which were calculated based on viscoelastic analyses considering the entire process cycle time, are compared to the ones from elastic analyses considering only the linear cool-down phase after the end of the cure process. The results show the elastic residual stresses that are always over-predicted ; this comes from the stress relaxation allowed in the viscoelastic analysis and the similar results can be found in White and Kim (1998) and Lee (2000).

Figure 4 shows that the hoop stress is maximum on $[(45/-45)_{2s}/90_4]$ compared to the other two stacking sequences. The elastic solutions for $[(15/-15)_{2s}/90_4]$, $[(30/-30)_{2s}/90_4]$, and $[(45/-45)_{2s}/90_4]$ result in 80%, 20%, and 10% higher values, respectively, than the viscoelastic. There are big differences in residual stresses between the aluminum liner and composites. Figure 5 shows the distribution of longitudinal stresses induced after the whole cure cycle. The largest longitudinal stress is found in $[(30/-30)_{2s}/90_4]$. The level of longitudinal stresses is similar to that of the hoop stresses partly because of perfect bonding at the interface between the liner and the composite. The elastic solutions with $[(15/15)_{2s}/90_4]$, $[(30/-30)_{2s}/90_4]$, and $[(45/-45)_{2s}/90_4]$ result in 29%, 11%, and 10% higher values, respectively, than the viscoelastic. The radial residual stresses are compressive and smaller as
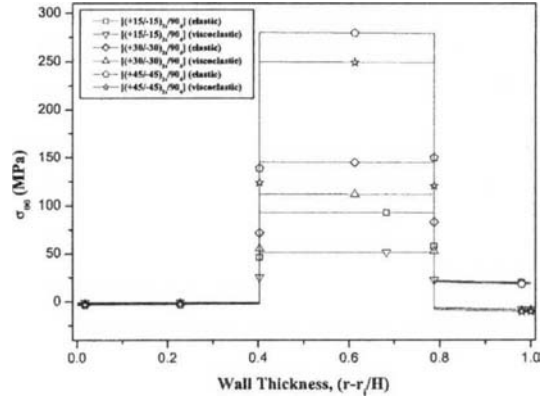

Fig. 4 Hoop residual stress distributions through the non-dimensionalized wall thickness at $z=0$ after cure
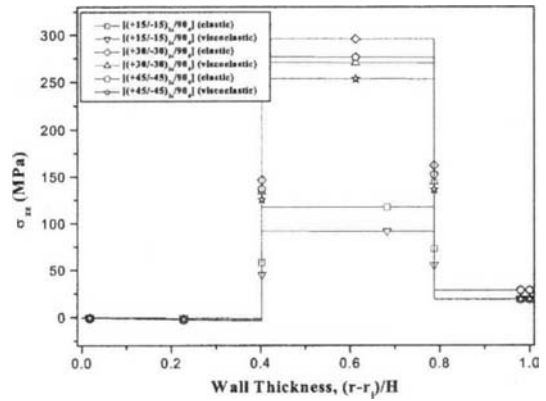

Fig. 5 Longitudinal residual stress distributions through the non-dimensionalized wall thickness at $z=0$ after cure
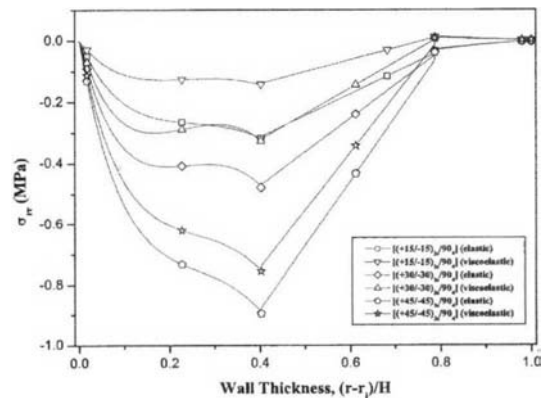

Fig. 6 Radial residual stress distributions through the non-dimensionalized wall thickness at $z=0$ after cure

shown in Fig. 6, compared to the other two stresses. The radial residual stresses are the highest at $[(45/ \quad -45)_{2s}/90_4]$. The elastic solutions for $[(15/-15)_{2s}/90_4]$, $[(30/30)_{2s}/90]$, and $[(45/-45)_{2s}/90_4]$ result in 110%, 50%, and 20% higher values, respectively than the viscoelastic. It is clear from these results that there is a need for including the viscoelastic effects of composite materials to predict residual stresses accurately.

Figures 7-9 illustrate the momentary development of residual stresses through the thickness of the cylinder wall at $z=0$ during the entire cure process. It can be easily seen from all these figures that the three residual stress components reach their own peaks at 180 minutes after the start of the curing process and then keeping constant through 240 minutes. This time span is coincident with when the cure of resin is almost 0.98 and then finally finished (i.e., 1.00) as shown in Fig. 3. Due to this the stresses are hard to be relaxed and entrapped at this moment. It is well known that during this period, most of mechanical properties are also built. Then, residual stresses are relaxed a little and remain in composite materials throughout cooling down. The low level of final residual stress is also observed in the aluminum liner and 90° layers compared with in the ±45° layers.

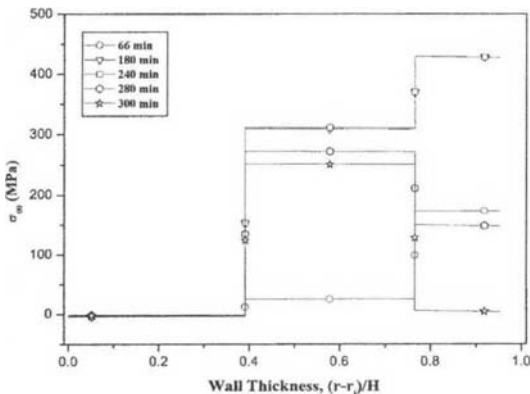Figures. 10 and 11 show the time-dependent hoop residual stresses of the $[(45/-45)_3]_s$ cylin-
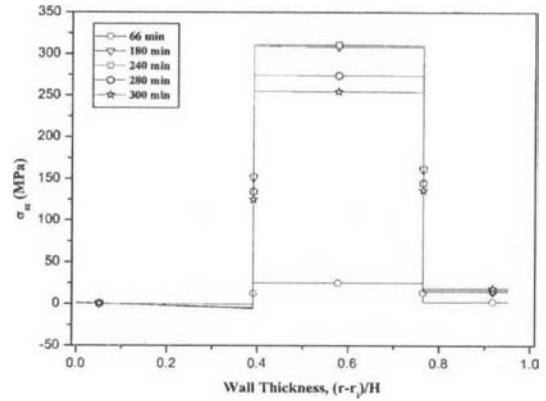

Fig. 8 Time-dependent longitudinal residual stress distributions of a $[(45/-45)_{2s}/90_4]$ cylinder at $z=0$ during cure
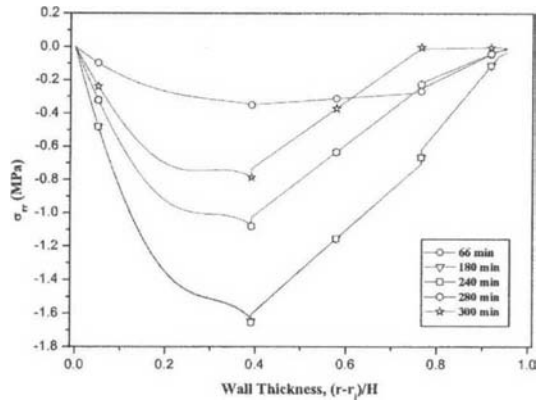

Fig. 9 Time-dependent radial residual stress distributions of a $[(45/-45)_{2s}/90_4]$ cylinder at $z=0$ during cure
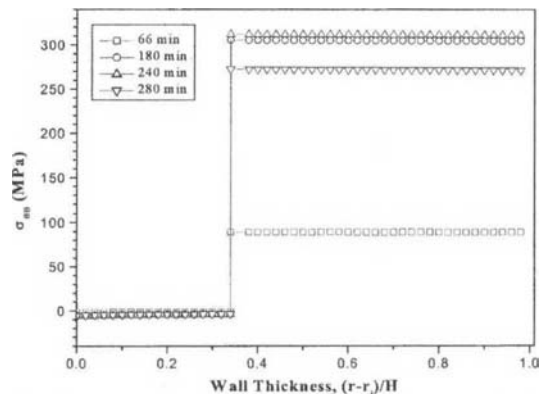

Fig. 7 Time-dependent hoop residual stress distributions of a $[(45/-45)_{2s}/90_4]$ cylinder at $z=0$ during cure

Fig. 10 Time-dependent hoop residual stress distributions of a $[(45/-45)_3]_s$ cylinder at $z=0$ during cure
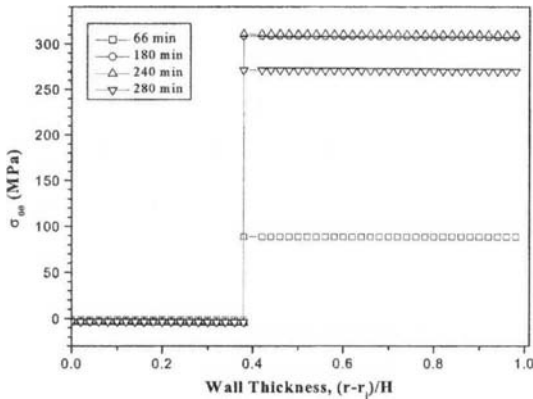
Fig. 11 Time-dependent hoop residual stress distributions of a $[(45/-45)_3]_s$ cylinder at $z=L/4$ during cure

der at two different longitudinal locations, $z=0$ and $L/4$ during cure. The small difference between two results indicates that residual stresses do not vary much along the cylinder during cure when the ends are free to move. Further studies on the other component of residual stresses along the cylinder during cure show similar trends and are not further depicted here.

7. Conclusions

In this study the thermo-viscoelastic residual stresses that occurred in the aluminum liner-inserted polymer composite cylinder were investigated during the cure cycle and after cure. The rocket motor case and fuselages are examples of such struture. The time and degree of cure dependent thermo-viscoelastic constitutive equations were developed and coupled with a thermo-chemical process model. These equations were solved with the finite element code developed to predict the residual stresses in the composite cylinder.

The results show that the elastic residual stresses are always over-predicted from 10% to 80% compared to the viscoelastic cases, depending on the winding pattern. Therefore, this result indicates that the viscoelastic effects should be considered for better prediction of residual stresses. Regardless of the winding patterns, it is always found that the highest difference of the residual

stresses exists between the aluminum liner and the polymer composite materials due to the mismatch of large thermal expansion coefficients. The hoop and radial residual stresses were the highest with $[(45/-45)_{2s}/90_4]$. However, the longitudinal residual stresses with $[(30/-30)_{2s}/90_4]$ were higher than the other two winding patterns. During cure, the highest residual stresses take place at the second dwell time and then decrease a little during cool-down. In addition, the residual stresses did not change much along the cylinder length except at the ends. A judicious choice of winding patterns should be made to lower the residual stress level to avoid any premature thermal buckling and matrix cracking.

Acknowledgment

References

Bogetti, T. A. and Gillespie, Jr. J. W., 1992, "Process-Induced Stress and Deformation in Thick-Section Thermoset Composite Laminate," *J. Composite Materials*, Vol. 26, pp. 626~660.

Christensen, R. M., 1982, *Theory of Viscoelasticity*, Academic Press, New York.

Hahn, H. T. and Pagano, N. J., 1975, "Curing Stress in Composite Laminates," *J. Composite Materials*, Vol. 9, pp. 91~105.

Kim, C. and White, S. R., 2001, "Continuous Curing and Induced Thermal Stresses of a Thick Filament Wound Composite Cylinder," *J. Reinforced Plastics and Composites*, Vol. 20, No. 2, pp. 166~181.

Kim, Y. K. and White, S. R., 1996, "Stress Relaxation Behavior of 3501-6 Epoxy Resin during Cure," *Polymer Eng. Sci.*, Vol. 36, pp. 2852~2862.

Lee, S. Y., 2000, "Curing Induced Residual Stresses in Laminated Cylindrical Shells," *KSME International Journal*, Vol. 14, No. 1, pp. 19~29.

Lee, W. I., Loos, A. C. and Springer, G. S., 1982, "Heat of Reaction, Degree of Cure, and

Viscosity of Herculus 3501-6 Resin," *J. Composite Materials*, Vol. 16, pp. 510~520.

Lin, K. Y. and Yi, S., 1991, "Analysis of Interlaminar Stresses in Viscoelastic Composites," *Int. J. Solids and Structures*, Vol. 27, pp. 929~945.

Taylor, R. L., Pister, K. S. and Goudreau, G. L., 1970, "Thermomechanical Analysis of Viscoelastic Solids," *Int. J. Numerical Methods in Eng.*, Vol. 2, pp. 45~59.

Vinson, J. R. and Sierakowski, R.L., 1987, *The Behavior of Structures Composed of Composite Materials*, Kluwer, Dordredcht, The Netherland.

Wang, A. S. D. and Crossman, F. W., 1977, "Edge Effects on Thermally Induced Stresses in Composite Laminates," *J. Composite Materials*, Vol. 11, pp. 300~312.

White, S. R. and Hahn, H. T., 1992, "Process Modeling of Composite Materials : Residual Stress Development during Cure. Part I. Model Formulation," *J. Composite Materials*, Vol. 26, No. 16, pp. 2402~2420.

White, S. R. and Kim, Y. K., 1998, "Process-Induced Residual Stress Analysis of AS4/3501-6 Composite Material," *Mechanics of Composite Materials and Structures*, Vol. 5, pp. 153~186.